Pflügers Arch – Eur J Physiol (1998) 436:679–688

ORIGINAL ARTICLE

Klaus W. Linz · Rainer Meyer

The late component of L-type calcium current during guinea-pig cardiac action potentials and its contribution to contraction

Received: 5 November 1997 / Received after revision: 12 June 1998 / Accepted: 15 June 1998

Abstract L-Type Ca^{2+} current ($I_{Ca,L}$) elicited during the action potential (AP) of guinea-pig ventricular myocytes exhibits an early and a late component. The whole-cell patch-clamp technique was used to characterize the process regulating the late $I_{Ca,L}$ component and to assess its contribution to excitation-contraction coupling. A stepwise decrease in repolarization rate of AP-like voltage-clamp pulses led to an exponential increase in Ca^{2+} charge carried by $I_{Ca,L}$. This saturation behaviour was significantly reduced or absent when Ba^{2+} or monovalent cations were used as charge carriers, which suggests that the late component of $I_{Ca,L}$ is controlled mainly by Ca^{2+}-dependent processes. Simultaneously recording $I_{Ca,L}$ and zero-load shortening or the internal Ca^{2+} concentration (fura-2) revealed that Ca^{2+} carried by the late component of $I_{Ca,L}$ markedly contributes to the Ca^{2+} content of the sarcoplasmic reticulum (SR). Reducing the charge transfer by late $I_{Ca,L}$ during a series of AP-like conditioning clamp pulses by 48% reduced the shortening amplitude during a subsequent test stimulation by 56%. This relationship was absent during long rectangular depolarizing conditioning clamps, during which Na^+/Ca^{2+} exchange increased its influence on SR Ca^{2+} loading. The late component of $I_{Ca,L}$ developed only a minor direct influence on the simultaneous cell shortening. Thus, the main contribution of the late $I_{Ca,L}$ component is to supply Ca^{2+} for SR loading.

Key words Action potential clamp · Ca^{2+}-dependent inactivation · Cell shortening · Excitation-contraction coupling · Fura-2 · Guinea-pig ventricular myocytes · L-Type current · SR Ca^{2+} content

K.W. Linz · R. Meyer (✉)
Physiological Institute, University of Bonn, Wilhelmstrasse 31, D-53111 Bonn, Germany
e-mail: meyer@physio.uni-bonn.de
Tel.: +49-228-2872311, Fax: +49-228-2872313

Introduction

Excitation-contraction coupling in cardiac myocytes is initiated by an influx of Ca^{2+}, mainly through L-type Ca^{2+}channels [7], or by a combination of $I_{Ca,L}$ and reverse Na^+/Ca^{2+} exchange [26]. During the upstroke and the early part of the action potential (AP), Ca^{2+} influx induces Ca^{2+} release from the sarcoplasmic reticulum (SR) [16]. The resulting rise of the internal Ca^{2+} concentration ($[Ca^{2+}]_i$), which controls the contraction of the myocyte, is directly related to the size of Ca^{2+} influx [32] and the amount of SR Ca^{2+} load [6, 41]. In a regularly beating myocyte, Ca^{2+} entering the cell during the AP plateau is removed before the subsequent contraction by Na^+/Ca^{2+} exchange [2, 42]. The extrusion of Ca^{2+} begins during the early plateau phase [15]. A change in the balance of inward and outward Ca^{2+} fluxes affects the Ca^{2+} content of the SR. It has been shown that prolongation of the AP leads to a net Ca^{2+} influx, which increases the SR Ca^{2+} loading thereby producing positive inotropic effects [6, 41]. This Ca^{2+} influx may pass through L-type Ca^{2+} channels [38], may be the result of reduced extrusion by Na^+/Ca^{2+} exchange [5, 32], or may be a combination of both [6, 12, 41].

Measurements by means of the AP clamp technique [13] have revealed that the time course of the L-type Ca^{2+} current ($I_{Ca,L}$) during an AP differs from that elicited by rectangular voltage-clamp steps [1, 6, 13, 18]. During an AP, $I_{Ca,L}$ inactivates much more slowly in a complex time course, depending on the species-specific AP. In guinea-pig ventricular myocytes, a fast early component can be distinguished from a slow late component lasting throughout the plateau phase [1, 13, 18].

The function of this late component of $I_{Ca,L}$ in excitation-contraction coupling in the heart has yet to be demonstrated. We therefore analysed the mechanism regulating this component of $I_{Ca,L}$ during an AP and quantified its contribution to SR Ca^{2+} loading and release. It could be shown that the amount of Ca^{2+} entering the cell during the late $I_{Ca,L}$ is correlated to the Ca^{2+} content of the SR, revealing its contribution to SR Ca^{2+} loading.

Materials and methods

Cell isolation

Ventricular myocytes from male guinea-pigs, weighing 250–400 g, were isolated enzymatically as previously described [30, 40]. Isolated cells were kept in oxygenated Tyrode's solution at 4°C for up to 8 h until use. Care and treatment of the animals was in accordance with the guidelines for care and use of laboratory animals in the *Deutsches Tierschutzgesetz*.

Electrophysiological recordings

Membrane currents were recorded at 35±1°C using the whole-cell mode of the patch-clamp technique [21]. Patch pipettes were pulled from borosilicate glass with a filament (Hilgenberg, Malsfeld, Germany). These had tip resistances of 2–4 MΩ when filled with the standard internal solution composed of (mM): KCl, 130; HEPES, 10 (pH 7.2 was obtained by addition of approximately 5 mM NaOH). A single-electrode continuous-voltage-clamp amplifier (L/M EPC7; List Medical Electronic, Darmstadt, Germany) was used. Cell capacitance, series resistance, and junction potentials were compensated by using the circuitry of the amplifier.

Membrane currents were elicited by rectangular voltage pulses, digitized APs ("AP clamp"), and combinations of rectangular voltage pulses and fast repolarizing voltage ramps ("AP-like clamps"). As command voltage for the AP clamp, digitized APs with overshoot amplitudes of 50 mV or 47 mV, and APD_{50}/APD_{90} of 350/380 ms or 375/450 ms, respectively, were used. These waveforms were characteristic for APs recorded in current-clamp mode under control conditions (overshoot amplitude: 45.4–52.1 mV, mean: 48.3±0.7 mV; APD_{50}: 193.3–446.5 ms, mean: 348.2± 47.5 ms; APD_{90}: 213.8–496.4 ms, mean: 377.8±52.3 ms; n=15). AP-like clamps were composed of a 50-mV square pulse of 50 ms duration followed by a descending ramp to –50 mV with variable slope (between –0.77 and –0.1 mV/ms). To achieve conditions favouring reverse-mode Na^+/Ca^{2+} exchange, in some experiments the square-pulse duration was increased from 50 to 365 ms. Stimulation frequency was set at 0.2 Hz or 1 Hz in the case of simultaneous shortening or $[Ca^{2+}]_i$ recordings. The holding potential was always –80 mV. Voltage-clamp pulses were designed to separate the L-type current from other current systems as follows:

1. The fast Na^+ current and the T-type Ca^{2+} current were inactivated by a 200-ms pre-clamp into the range of –40 to –35 mV. In some recordings the Na^+/Ca^{2+} exchange was blocked by substituting Li^+ for Na^+ in the external and internal solutions [14, 17, 23].
2. The L-type current was determined as that sensitive to 100 µM Cd^{2+} or 1 µM dihydropyridine (PN200-110) (see [12]).

K^+ currents were not blocked by substitution of K^+ for impermeable cations in the recording solutions, since this has been shown to reduce the L-type current significantly [30] and to influence excitation-contraction coupling [29, 43]. The method of difference-current recording is sensitive to changes in outward currents, which lead to a difference current that is not equal to the Cd^{2+}-sensitive current. Therefore, current records exhibiting difference currents at potentials at which the L-type current is not activated, e.g. at the end of the pre-clamp or at the holding potential, were discarded.

Cell capacitance was calculated routinely for every cell prior to capacitance compensation from the capacitive current elicited by a fast ramp clamp from –40 to –50 mV (slope: 5.5 mV/ms).

Optical shortening recordings

The phasic contraction of single cells was recorded optically as unloaded shortening [36]. With this method relative changes in cell length could be measured while electrophysiological recordings were being made.

Recordings of $[Ca^{2+}]_i$

Intracellular Ca^{2+} transients were measured in voltage-clamped cells pre-incubated for 20 min at 35°C in Tyrode's solution containing 1 µM fura-2/AM (Molecular Probes, Eugene, Ore., USA). To prevent loss of dye by cell dialysis via the patch-clamp electrode, 75 µM fura-2 pentapotassium-salt (Molecular Probes) was added to the internal solution. Following fura-2 incubation cells were kept in normal Tyrode's solution at 35°C for 30 min to allow dye conversion. Fura-2 fluorescence [19] was recorded by means of a fast fluorescence microphotometry system (Zeiss FFP attached to a Zeiss IM 35 microscope with Zeiss Ultrafluar 100× objective; Carl Zeiss, Jena, Germany) synchronized to the patch-clamp setup. Fura-2 excitation (340 and 380 nm) was performed with 16 ms time resolution. Fluorescence emission (420–560 nm) of the patch-clamped cell was recorded by a photomultiplier tube (1.6 mm aperture covering 10 µm in the object plane). Changes in $[Ca^{2+}]_i$ were determined as the ratio of the emitted fluorescence.

Rapid perfusion system

For rapid changes of the superfusate around the investigated cell, a custom-made heated solution-switcher was used. This system was constructed following the description of Levi et al. [28]. The average time for complete change of solution, estimated from open pipette experiments, was 60 ms.

Data analysis and statistics

Voltage-clamp protocols, data acquisition and data storage were accomplished using pClamp 6.0 (Axon Instruments, Foster City, Calif., USA).

$I_{Ca,L}$ peak-current/voltage (I/V) relations obtained from measurements with rectangular voltage-clamp pulses were fitted as published elsewhere [30]. For averaging data from different cells, membrane currents were normalized to the cell capacitance. In the case of shortening, data recordings were normalized to the amplitude measured under control conditions. All values are reported as means ± SD; n is the number of cells. Error bars in figures represent SD. The statistical significance of relative changes was tested using unpaired Student's t-test or one-way ANOVA. Differences with $P<0.05$ were regarded as significant.

Solutions

The external solutions for patch-clamp measurements were based on Tyrode's solution which was composed of (mM): NaCl, 135; KCl, 4; $CaCl_2$, 1.8; $MgCl_2$, 1; glucose, 11; HEPES, 2 (pH 7.2 with NaOH). For measurements of Ba^{2+} carried L-type current ($I_{Ba,L}$) $BaCl_2$ was substituted for an equimolar amount of $CaCl_2$. To record non-selective cation currents through the L-type channels ($I_{ns,L}$) 2.5 mM EGTA was added to a Ca^{2+}-free Tyrode's solution [21, 22, 33]. To prevent changes in surface potential Mg^{2+} was substituted for Ca^{2+} in the external solution. Since the presence of divalent cations markedly reduces $I_{ns,L}$ 1 µM isoprenaline (*N*-isopropyl-DL-noradrenaline-hydrochloride; Fluka, Buchs, Switzerland) was added to the external solution to compensate for this [33]. In control recordings Li^+ was substituted for Na^+ ("Li^+-Tyrode") to block Na^+/Ca^{2+} exchange [14, 17, 23]. To block the L-type current for determination of difference current 100 µM Cd^{2+} or 1 µM PN200-100 (Isradipine; Research Biochemicals International, Natick, Mass., USA) was added to the Tyrode's solution.

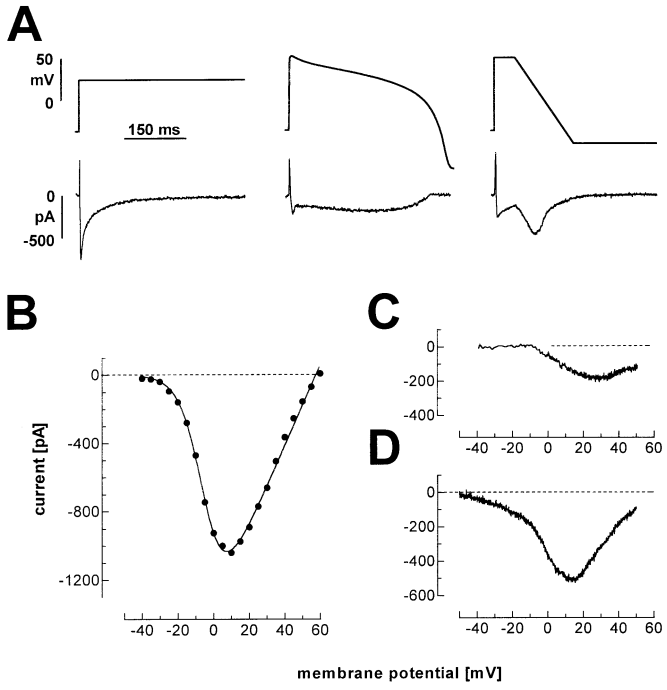

Fig. 1A–D Recordings of L-type Ca^{2+} current ($I_{Ca,L}$) using rectangular clamps, digitized action potentials (*AP clamps*), and combinations of rectangular voltage pulses and fast repolarizing voltage ramps (*AP-like clamps*) as command voltage. All recordings were obtained from the same cell. The results are typical for measurements made from ten other cells. **A** Original recordings of Cd^{2+}-sensitive current (*lower panels*) obtained using the voltage clamp protocols plotted in the *upper panels*. All clamp pulses were preceded by a pre-clamp to –35 mV (not shown). The amplitude of the rectangular clamp pulse was 25 mV, corresponding to the potential range in the middle of the AP plateau. The AP-like clamp consisted of a rectangular clamp to 50 mV (duration: 50 ms) followed by a repolarizing ramp to –50 mV (slope: 0.77 mV/ms). **B–D** Current/voltage (*I*/*V*) relationships determined from the recordings shown in **A**. **B** Peak *I*/*V* relation of $I_{Ca,L}$ elicited by rectangular clamps graded in 5-mV steps. **C** Continuous *I*/*V* relation of $I_{Ca,L}$ during the AP clamp. **D** Continuous *I*/*V* relation of $I_{Ca,L}$ during the AP-like clamp

Results

Time course of L-type Ca^{2+} current during rectangular, AP-shaped, and AP-like clamps

To characterize the $I_{Ca,L}$ in our preparation we performed voltage-clamp measurements using rectangular, AP-shaped, and AP-like clamp protocols on the same cells. Figure 1 shows an example of such an experiment. During a rectangular voltage-clamp pulse, the $I_{Ca,L}$ exhibited the classic time course, with rapid activation followed by bi-exponential inactivation (Fig. 1A, left panel). The peak current values followed the typical U-shape when plotted against membrane potential (Fig. 1B), with a maximum inward current of –11.97±0.13 pA/pF (*n*=11) at 10 mV. Fitting of the *I*/*V* relationships revealed a reversal potential of 59.8±0.5 mV (*n*=11).

In contrast to rectangular voltage clamps, the $I_{Ca,L}$ during an AP clamp showed a complex time course with a characteristic separation into a fast early and a sustained late component (Fig. 1A, middle panel). In order to distinguish the early from the late component of $I_{Ca,L}$ in a defined way, the current traces were differentiated and the time when d*I*/d*t* reaches its first local minimum was determined. The early component activated within 4.3±0.4 ms (*n*=11) and decayed again after 12.4±1.4 ms (*n*=11). This partial inactivation was followed by the late component of $I_{Ca,L}$ which lasted throughout the AP plateau. In some cells the $I_{Ca,L}$ slightly increased again during this time (as is the case in Fig. 1A) while in others it stayed nearly constant or decayed very slowly (see Fig. 4A). At the beginning of the repolarization phase $I_{Ca,L}$ ceased completely. A comparison of the charge carried by the early and by the late component demonstrated that 5.9±1.4% (*n*=11) of the total charge entering the cell through L-type channels during an AP is carried by the early $I_{Ca,L}$.

A more distinct separation of early and late components was achieved by means of AP-like voltage-clamp pulses comprising a short rectangular clamp to 50 mV and a fast repolarizing ramp to –50 mV (Fig. 1A, right panel). During the square pulse the $I_{Ca,L}$ became partially activated, showing characteristics analogous to the early component during an AP clamp. The subsequent ramp clamp activated an even greater amount of $I_{Ca,L}$ leading to a second maximum of inward current. This late component decreased to zero during ongoing repolarization to –50 mV.

By plotting the current values of the late component continuously as a function of clamp potential, *I*/*V* relationships for the late component could be constructed (Fig. 1C, D). In the case of AP-like clamps, these curves were U-shaped. For AP clamps, U-shaped to linear *I*/*V* relationships were observed. In contrast to the peak *I*/*V* curves obtained by rectangular clamp protocols, the maximum value was shifted to more positive potentials and the current amplitude was significantly smaller. During an AP clamp a maximum late current of –1.68±0.24 pA/pF was reached at 41.3±6.9 mV (*n*=11). However, the potential of maximum late current varied over a relatively wide range depending on whether $I_{Ca,L}$ increased a second time during the late component (see above). During application of an AP-like clamp with a slope of 0.77 mV/ms, the maximum late $I_{Ca,L}$ was –3.77±0.07 pA/pF at 19.5± 2.4 mV (*n*=11).

Determination of L-type Ca^{2+} current as Cd^{2+}- or PN200-110-sensitive current

The $I_{Ca,L}$ was routinely determined as difference current. Therefore, each measurement consisted of two successive recordings, the first one under control conditions and the second after block of L-type channels by application of 100 µM Cd^{2+} or 1 µM PN200-110. The current recorded in the presence of the blocking agent was subtracted from the total membrane current recorded in the absence of blocking agents (Fig. 2A). Usually Cd^{2+} was

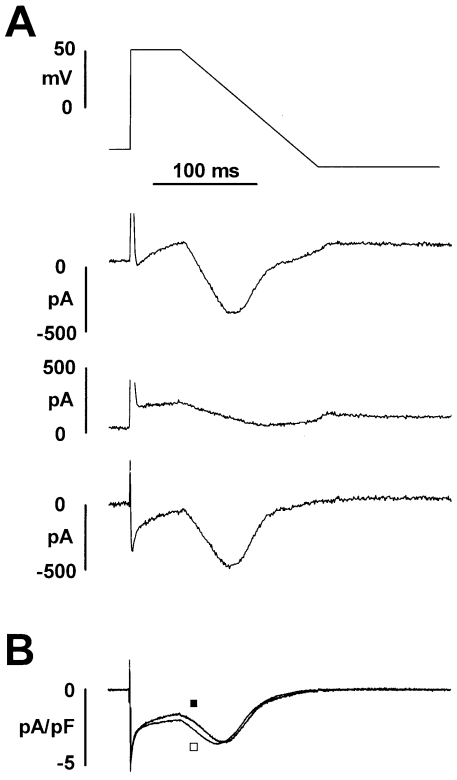

Fig. 2A, B Recordings of difference current during AP-like clamps. **A** Determination of Cd^{2+}-sensitive difference current. *Top panel*: voltage-clamp protocol consisting of a rectangular clamp to 50 mV (duration: 50 ms) followed by fast repolarizing ramp to –50 mV (slope: 0.77 mV/ms). *Second panel*: example of total membrane current recorded in the absence of channel blockers. *Third panel*: membrane current recorded in the presence of 100 µM Cd^{2+}. Recording is from the same cell as in the *second panel*. *Bottom panel*: Cd^{2+}-sensitive difference current calculated by subtracting the trace shown in the *third panel* from the trace shown in the *second panel*. **B** Normalized 100 µM Cd^{2+}-sensitive current recorded under control conditions (■) and after inhibition of Na^+/Ca^{2+} exchange by complete substitution of Li^+ for Na^+ (□). The *traces* represent the average of recordings from 8 cells. Command voltage was the same as shown in **A**

used to block the L-type channels, since the dihydropyridine showed significant use dependence, leading to an underestimation of L-type current. The difference current might be contaminated by currents other than $I_{Ca,L}$. In particular, current carried by Na^+/Ca^{2+} exchange (I_{NaCa}) could contribute to the difference current, when I_{NaCa} markedly changes due to the change in the intracellular Ca^{2+} transient after block of $I_{Ca,L}$. In control experiments this possible source of artefacts was investigated. Figure 2B shows a comparison of AP-like clamp recordings of the 100 µM Cd^{2+}-sensitive current under standard conditions and after block of Na^+/Ca^{2+} exchange by substituting Li^+ for Na^+ in the external and internal solutions [14, 17, 23]. In the absence of I_{NaCa} the difference current was slightly increased. These experiments demonstrate that the Cd^{2+}-sensitive current is carried mainly via L-type channels and that the Na^+/Ca^{2+} exchanger does not contribute appreciably to this current (see also Fig. 3F). In the case of active Na^+/Ca^{2+} exchange, the difference current was only slightly smaller than after Li^+ block. Thus, $I_{Ca,L}$ determined as Cd^{2+}-sensitive current might be slightly underestimated. Even during very long depolarizing rectangular voltage-clamp pulses (50 mV, 365 ms), which strongly favour reverse Na^+/Ca^{2+} exchange, the difference current determined after Li^+ block of I_{NaCa} differed only slightly from that under control conditions (see Fig. 7A and discussion in the text).

Control of the late component of $I_{Ca,L}$

The use of AP-like clamps offers the possibility to simulate changes in the AP course in a defined way. In addition, this clamp protocol permits a clear separation of the early and late components of $I_{Ca,L}$. The following set of experiments was designed to analyse and explain the time course of the late $I_{Ca,L}$ component during the AP-like clamps. We used a clamp protocol in which the repolarization rate was systematically reduced from 0.77 to 0.1 mV/ms by increasing the duration of the repolarizing ramp (Fig. 3A). With increasing ramp duration the course of the late current changed significantly (Fig. 3B). During the shortest ramp, the $I_{Ca,L}$ rapidly increased, reaching a peak value which was higher than the peak of the early component, and thereafter decreased rapidly (see Fig. 1A). Prolonging the ramp duration reduced the amplitude of the late $I_{Ca,L}$ component. Moreover, the latter became less pronounced. During the two longest ramps the late current decreased almost linearly. By integrating the original current records over time, the charge carried by $I_{Ca,L}$ could be calculated (Fig. 3F). During the shortest ramp the net charge carried by $I_{Ca,L}$ was 178.8±5.9 fC/pF (n=34). With increasing ramp duration the amount of charge flow increased exponentially. The maximum charge transfer as calculated by a monoexponential fit was 2.6±0.1 times the value measured during the steepest ramp. Since the driving force for Ca^{2+} increases linearly with progressing repolarization during the ramp clamp, the saturation behaviour of late $I_{Ca,L}$ points towards a control of this current component by inactivation and/or deactivation of L-type channels. Similar results were also obtained when Na^+/Ca^{2+} exchange was blocked by substituting Li^+ for Na^+ (Fig. 3C). However, comparable to the results shown in Fig. 2B, current amplitude and charge transfer were slightly increased in the absence of Na^+/Ca^{2+} exchange. In Na^+-free solutions the net charge carried during the steepest ramp was 195.4± 21.1 fC/pF (n=8). With rising ramp duration it increased exponentially to an upper limit of 2.9±0.1 (n=8) times the starting value.

It is known from previous experiments with rectangular voltage-clamp protocols that the process of L-type channel inactivation is dependent on voltage and Ca^{2+} [3, 10, 20, 24, 25]. To distinguish between the voltage- and Ca^{2+}-dependent processes, we substituted Ca^{2+} as charge carrier with Ba^{2+} or monovalent cations; it has previously been shown that Ba^{2+} current through L-type channels ($I_{Ba,L}$) exhibits a markedly reduced, though not complete-

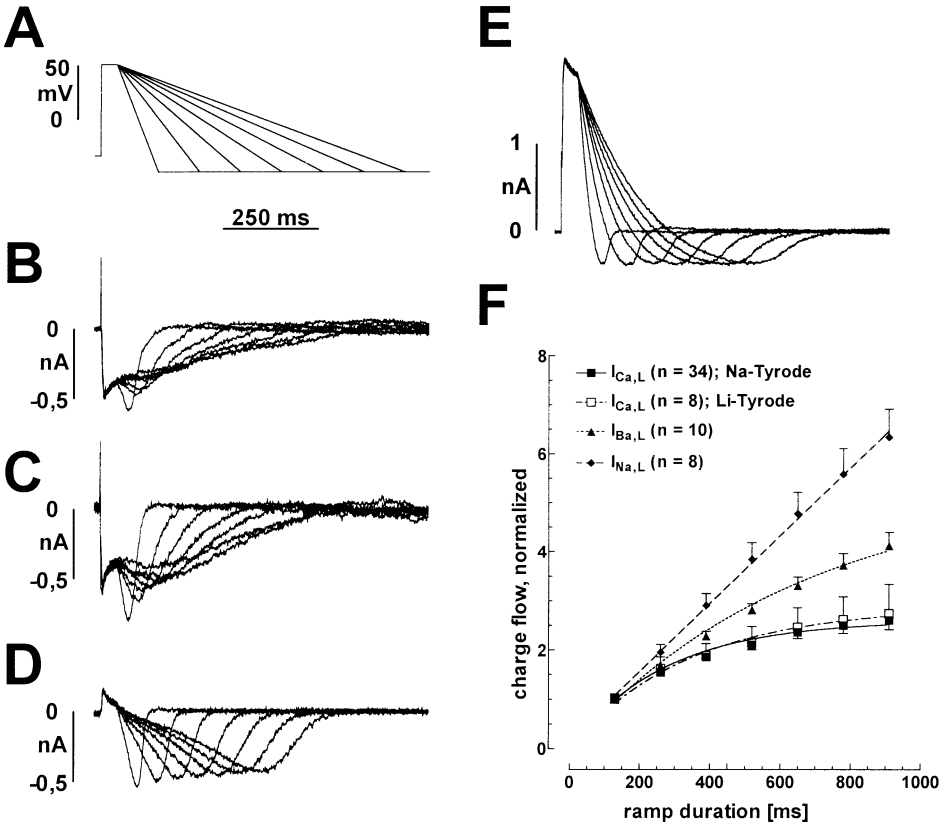

Fig. 3A–F Recordings of L-type current elicited by AP-like clamps using different charge carriers. **A** Voltage-clamp protocol consisting of a rectangular clamp to 50 mV (duration: 50 ms) followed by fast repolarizing ramps to –50 mV (slope decreasing from 0.77 to 0.1 mV/ms). **B–E** Original recordings of L-type current elicited by the protocol shown in **A**. As charge carriers, Ca^{2+} ($I_{Ca,L}$; **B**, **C**), Ba^{2+} ($I_{Ba,L}$; **D**), and monovalent cations ($I_{ns,L}$; **E**) were used. For the recordings in **B**, **D**, and **E**, Na^+-based Tyrode's solutions were used. For the recording shown in **C** the Tyrode was Na^+-free ("Li-Tyrode"). Recordings are from different cells. **F** Normalized charge flow through L-type channels as a function of ramp duration. Data points were calculated by integrating the original current traces over time. In the case of $I_{Ba,L}$ and $I_{Na,L}$ the charge flow equals the sum of charge carried in the outward and inward directions. The data for $I_{Ca,L}$ and $I_{Ba,L}$ were fitted by means of monoexponential functions. The data for charge carried by $I_{ns,L}$ were fitted by linear regression

ly absent, charge-dependent inactivation [9, 34], whereas monovalent cation current through L-type channels ($I_{ns,L}$) exhibits only voltage-dependent inactivation [20]. In the present experiments, using rectangular voltage-clamp pulses the inactivation time course of $I_{Ba,L}$ was markedly slowed, while $I_{ns,L}$ exhibited only small time-dependent inactivation (data not shown). The reversal potential for the peak $I_{Ba,L}$ and $I_{ns,L}$ was 44.9±0.3 mV (n=20) and 14.5±0.7 mV (n=18), respectively. Using AP-like clamps, an early and a late component of L-type current could be separated into $I_{Ba,L}$ and $I_{ns,L}$, as in the case of $I_{Ca,L}$ (Fig. 3D, E). With both charge carriers the early component was outwardly directed due to the reversal potentials. Moreover, the late component was more pronounced, as in the case of $I_{Ca,L}$. The decrease in peak amplitude of the late component of $I_{Ca,L}$ due to reduction in repolarization rate was less obvious when using Ba^{2+} as a charge carrier and absent for $I_{ns,L}$. The total charge fluxes carried through the L-type channels were calculated as for the $I_{Ca,L}$ (Fig. 3F). During the steepest ramp the total charges carried by $I_{Ba,L}$ and $I_{ns,L}$ were 202.8±6.5 fC/pF (n=10) and 393.1±32.7 fC/pF (n=8), respectively. The relationship between Ba^{2+} charge flow and the duration of the repolarizing ramps followed an exponential course, reaching an upper limit which was 5.4±0.3 times higher than the starting value. In contrast, the flux of monovalent cations did not saturate but increased linearly with increasing ramp duration. These results correlate with the different abilities of the substitute charge carriers to induce charge-dependent inactivation of L-type channels, and lead to the conclusion that the charge flow of the late component of $I_{Ca,L}$ during AP-like clamps is controlled mainly by a Ca^{2+}-dependent process. However, the measurements of $I_{ns,L}$ showed that, in the absence of Ca^{2+}-dependent inactivation, an additional voltage-dependent process (presumably deactivation of L-type channels, i.e. voltage-dependent closing of their activation gates) decreased the L-type current during repolarization (Fig. 3E).

Influence of the late component of $I_{Ca,L}$ on phasic contraction

To investigate the influence of the late $I_{Ca,L}$ component on excitation-contraction coupling we performed mea-

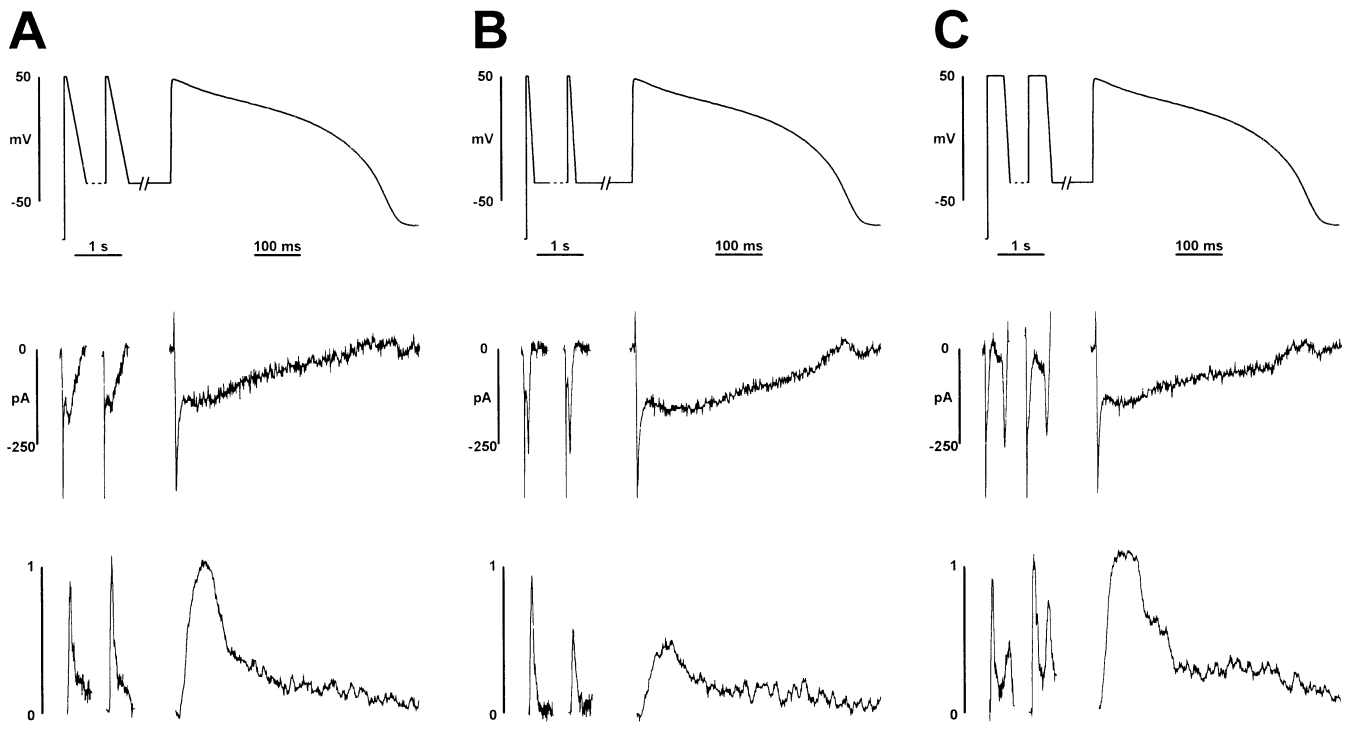

Fig. 4A–C Influence of the late $I_{Ca,L}$ component on sarcoplasmic reticulum (*SR*) Ca^{2+} loading. Cell shortening recordings. Voltage-clamp protocols (*upper panel*) consisting of ten consecutive AP-like conditioning clamps (only the first and the tenth are shown) and an AP-shaped test-clamp (stimulation frequency: 1 Hz) were used. Three different AP-like clamp patterns were applied subsequently to the same cell. **A** A 50-ms square pulse followed by a long repolarizing ramp (repolarization rate: 0.2 mV/ms). **B** A 50-ms square pulse combined with a short repolarizing ramp (0.77 mV/ms). **C** Combination of a 365-ms square pulse and a short repolarizing ramp (0.77 mV/ms). *Middle panels*: original traces of $I_{Ca,L}$. During the AP clamp a clear separation of early and late $I_{Ca,L}$ can be seen. The slower decrease in late inward current during the test clamp shown in **B** was regularly observed. These differences can be also expressed by the charges carried by $I_{Ca,L}$ which were 276.4±48.9 fC/pF, 386.1±64.7 fC/pF, and 282.0±56.7 fC/pF (n=17) for the conditions shown in **A**, **B**, and **C**, respectively. This might reflect less Ca^{2+}-dependent inactivation of $I_{Ca,L}$ due to a reduced intracellular Ca^{2+} transient. *Bottom panels*: recordings of cell shortening. The *traces* are displayed as relative signals normalized to the shortening amplitude obtained during the test clamp following the long AP-like clamp. Similar recordings were made from 16 other cells

surements of cell shortening during AP-shaped and AP-like clamps. In the first set of experiments the influence of the late current on SR Ca^{2+} content was investigated. Myocytes were conditioned by a train of ten identical AP-like clamps to obtain a steady-state in SR Ca^{2+} loading. For each cell the effects of conditioning pulses with long ramps (repolarization rate: 0.2 mV/ms; Fig. 4A) and short ramps (0.77 mV/ms; Fig. 4B) were compared. The charge carried by $I_{Ca,L}$ during these clamp protocols differed by a factor of 0.48, or by 0.47 when Na^+/Ca^{2+} exchange was blocked by Na^+-free solutions (Fig. 7A; see also Fig. 3F). In the case of the short and the long ramps, the conditioning train was followed by the same AP-shaped test clamp. Cell shortening elicited during this clamp was used as an approximation of the SR Ca^{2+} content built up by the conditioning clamps. Recordings in the lower panels of Fig. 4 show that the shape of the conditioning pulses influenced the charge carried, as well as the shortening amplitude during the AP-shaped test clamp. By decreasing the ramp duration of the conditioning AP-like clamps, the cell shortening was reduced to 56% which is within the same range as the reduction of Ca^{2+} charge flow (P=0.1 tested by Student's t-test; Fig. 7A). This correlation points towards a marked influence of the Ca^{2+} entering the cell through L-type channels during the AP plateau on the Ca^{2+} content of the SR. In contrast to the amplitude, the rise time of the shortening signal was not significantly influenced by the shape of the conditioning pulses. Increasing the repolarization rate changed the time to peak values from 107.7±27.3 ms to 120.1±32.9 ms (n=17; P=0.2).

In order to investigate the influence of the Na^+/Ca^{2+} exchange on SR Ca^{2+} loading, conditioning clamps favouring Ca^{2+} influx via reverse-mode Na^+/Ca^{2+} exchange were created by combining a long-lasting square pulse (duration: 365 ms) with the short repolarizing ramp (slope: 0.77 mV/ms; Fig. 4C). The $I_{Ca,L}$ elicited by this clamp pattern was characterized by a marked delay between the fast and late current components, which led to double-peak contractions. An almost identical time course of $I_{Ca,L}$ was obtained when the difference current was recorded after block of Na^+/Ca^{2+} exchange by substituting Li^+ for Na^+ (n=8). This indicates that the late inward hump of difference current is due to $I_{Ca,L}$ and not an artefact due to changes in I_{NaCa}. The prolongation of the depolarizing square pulse led to a reduction of charge carried by $I_{Ca,L}$ to 75% (73% in Na^+-free solutions) com-

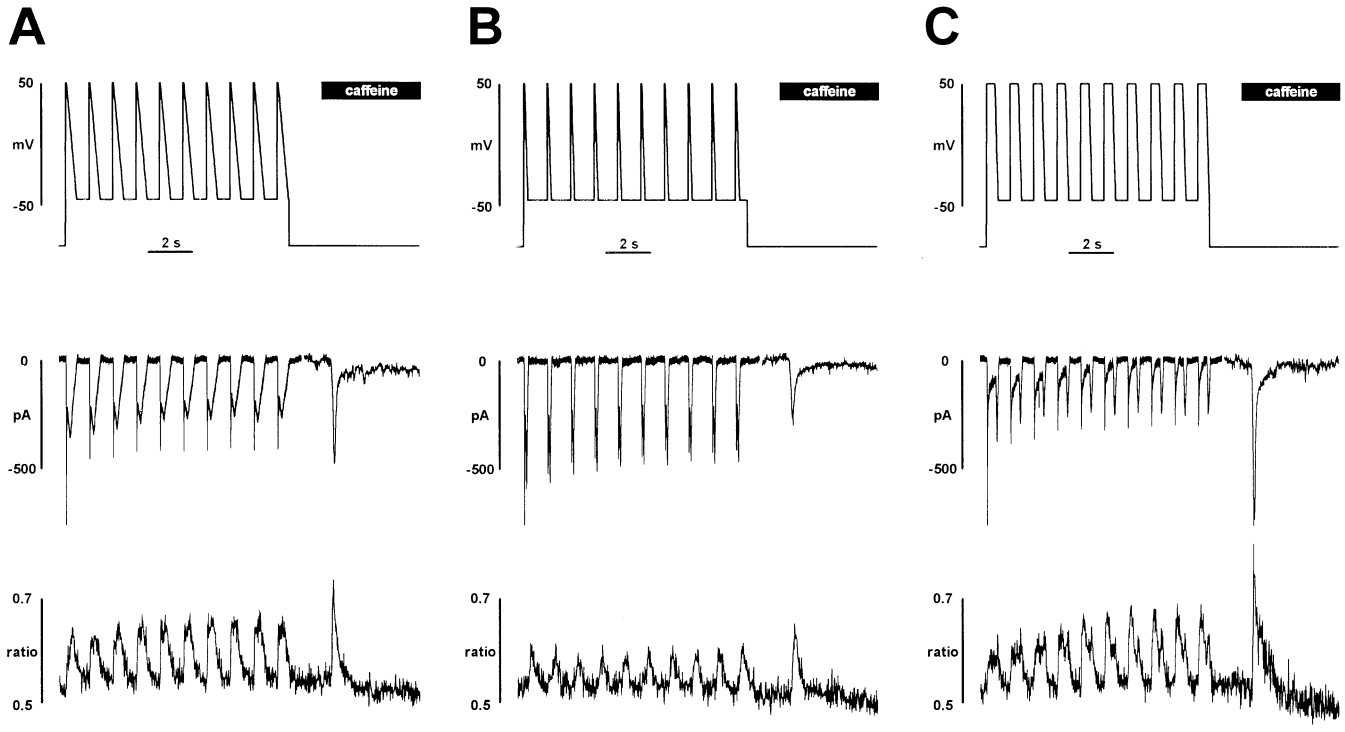

Fig. 5A–C Influence of the late $I_{Ca,L}$ component on SR Ca^{2+} loading. Recordings of $[Ca^{2+}]_i$. As in the experiments of Fig. 4, ten consecutive AP-like clamp pulses were used for cell conditioning (*upper panels*). Instead of a test clamp, the membrane potential was held at –80 mV during the subsequent period and the cells were exposed to a pulse of 10 mM caffeine for the time indicated by the *black bar* (5 s duration after 1 s delay) in order to discharge the SR. Three different conditioning-clamp patterns were applied subsequently to the same cell. **A** A 50-ms square pulse followed by a slow repolarizing ramp (0.2 mV/ms). **B** A 50-ms square pulse combined with a fast repolarizing ramp (0.77 mV/ms). **C** Combination of a 365-ms square pulse and a slow repolarizing ramp (0.77 mV/ms). *Middle panels*: original traces of total membrane current after subtraction of leak current. In order to assess the Na^+/Ca^{2+} exchange-carried compensation current of caffeine discharge, the total membrane current, but not the Cd^{2+}-sensitive current, was analysed. For technical reasons the current during caffeine discharge was sampled with lower time resolution. The high inward peak current amplitude observed in each case during the first AP-like clamp was due to activation of fast I_{Na}. *Bottom panels*: recordings of changes in $[Ca^{2+}]_i$ using fura-2. The ratio 340/380 nm is displayed. Similar recordings were made from eight other cells

pared to the conditioning clamp with the long repolarizing ramp (Fig. 7A). In contrast, the shortening amplitude measured during the AP-shaped test clamp had increased to 110%. Thus, under conditions favouring the reverse-mode of the Na^+/Ca^{2+} exchange, the relationship between charge carried by $I_{Ca,L}$ and SR Ca^{2+} content is not proportional.

In addition to the cell-shortening measurements, we tried to assess the degree of SR loading also using a more direct approach. Myocytes were voltage clamped with the same conditioning clamp protocols that were used for the shortening recordings. However, instead of the AP-shaped test clamp, the cells were clamped to –80 mV and after an interval of 1 s 10 mM caffeine was applied for 5 s by means of a rapid solution switcher in order to completely discharge the SR [39]. Changes in $[Ca^{2+}]_i$ were monitored using fura-2. As can be seen from Fig. 5, both the $[Ca^{2+}]_i$ transient and the compensation current (total membrane current after leak subtraction) during caffeine discharge strongly depend on the course of the conditioning clamps. The time integral of the $[Ca^{2+}]_i$ transient elicited by caffeine was related to the conditioning clamp in the same way as the shortening amplitude (Fig. 7A). Thus, under our experimental conditions SR loading and shortening amplitude elicited by the test clamp are directly correlated.

In a second approach possible effects of the late component of $I_{Ca,L}$ on triggering and time course of the cell shortening were tested. The voltage-clamp protocol consisted of ten identical AP clamps as conditioning pulses to achieve a constant SR loading, and the two AP-like clamps, which had been used for cell conditioning in the experiments shown in Fig. 3A, B, were used as test clamps (Fig. 6). In contrast to the noticeable changes in shortening amplitude observed when the AP-like clamps were used to adjust the SR Ca^{2+} content, the cell contraction was not significantly influenced by the course of the late $I_{Ca,L}$ component during the test clamp (Fig. 6, bottom traces, and Fig. 7B). Likewise, the rise time of cell shortening had only slightly increased when the duration of the repolarizing ramp was decreased. The time for 10% to 90% decay of the shortening signal became significantly less when the repolarization rate of the AP-like clamp was reduced. However, from these experiments it is not possible to distinguish whether this is due to the increased Ca^{2+} influx via the late $I_{Ca,L}$, an increased reverse (or reduced forward) Na^+/Ca^{2+} exchange during the lon-

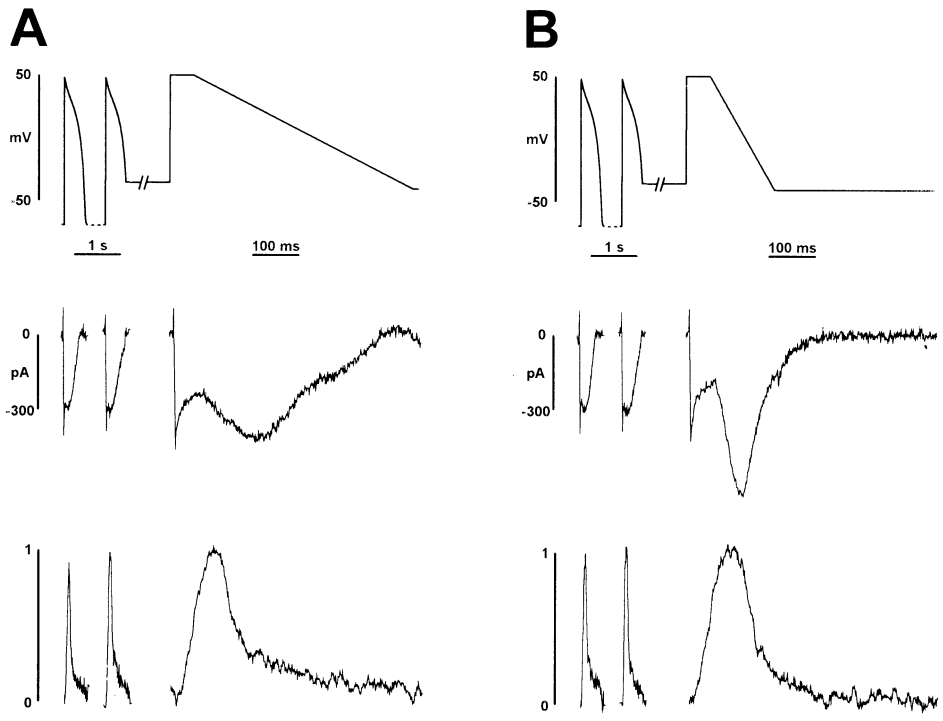

Fig. 6A, B Influence of the late $I_{Ca,L}$ component on triggering and time course of contraction. The voltage clamp protocols (*upper panels*) consisted of ten consecutive AP-shaped conditioning clamps (only the first and the tenth are shown) and an AP-like test clamp (stimulation frequency: 1 Hz). AP-like clamps with a 50-ms square pulse and repolarization rates of 0.2 mV/ms (**A**) and 0.77 mV/ms (**B**) were applied. In the *middle panels* the original traces of $I_{Ca,L}$ and in the *bottom panels* the relative cell shortening, from the same cell, are shown. The signals were normalized as described in Fig. 4. Similar results were obtained from 14 cells

ger ramp, or both. In summary, the late component of $I_{Ca,L}$ did not influence the triggering and the rising phase of the actual cell contraction but might have had some influence on the time course of relaxation.

Discussion

Control of the late $I_{Ca,L}$ component during an AP

AP clamp studies of guinea-pig [1, 13, 18, 41] and rat ventricular myocytes [6, 12] have revealed that the $I_{Ca,L}$ during an AP differs substantially from that during a rectangular voltage-clamp pulse. During a guinea-pig AP, the $I_{Ca,L}$ exhibits a fast early and a sustained late component (see Fig. 1A). The course of the late $I_{Ca,L}$ during the AP plateau is thought to be determined by the balance of increasing driving force for Ca^{2+} on the one hand and progressive inactivation of L-type channels on the other [1]. Inactivation of $I_{Ca,L}$ is a voltage- and Ca^{2+}-dependent process [10, 20, 24, 25]. However, the relative contribution of these two components to channel inactivation during an AP remains uncertain [8, 35]. The time course of the late component of the $I_{Ca,L}$ during the AP-like clamps in this investigation varied, depending on the steepness of the repolarizing ramps. We tried to find an explanation for this behaviour by the use of different charge carriers. The slowing of the repolarization rate, which resembles an increase in AP duration, led to a saturation of Ca^{2+} influx by $I_{Ca,L}$ (Fig. 3). This saturation behaviour of L-type current could be completely eliminated by replacing Ca^{2+} with monovalent cations as the charge carrier, which abolished the Ca^{2+}-dependent, or more exactly the charge-dependent, component of L-type channel inactivation. It thus seems that the Ca^{2+}-dependent component of L-type channel inactivation is the fundamental parameter that counterbalances the increasing driving force for Ca^{2+} during repolarization. Ca^{2+}-dependent L-type channel inactivation increases with progressing repolarization and thereby determines the $I_{Ca,L}$ during an AP-like clamp. Moreover, the Ca^{2+}-dependent component of inactivation represents a negative feedback mechanism that limits the Ca^{2+} influx during the AP-like clamp to a maximum value, even when repolarization is greatly delayed (Fig. 3F).

Influence of the late component of $I_{Ca,L}$ on SR Ca^{2+} load and phasic contraction

AP clamp measurements made from rat [6, 12] and guinea-pig [41] ventricular myocytes have demonstrated that an increase in AP duration has a strong positive inotropic effect. In contrast to a prolongation of rectangular voltage-clamp steps, increasing the AP duration will lead to an additional charge transfer carried by the late component of $I_{Ca,L}$ (see Fig. 3F). Nevertheless, longer APs may also lead to diminished Ca^{2+} outward transfer or increased Ca^{2+} inward transfer by the Na^+/Ca^{2+} exchanger. Both mechanisms, the late component of $I_{Ca,L}$ and the Na^+/Ca^{2+} exchange, may thus contribute to SR Ca^{2+} load. We could demonstrate that in guinea-pig the SR Ca^{2+} content correlates with Ca^{2+} influx through L-type channels. Halving the Ca^{2+} entry through L-type channels during a train of conditioning clamps reduced cell shortening during the test clamp by nearly 50% and the intracellular Ca^{2+} transient following caffeine discharge by more than 40% (Fig. 7A). Thus, besides variations in Na^+/Ca^{2+} ex-

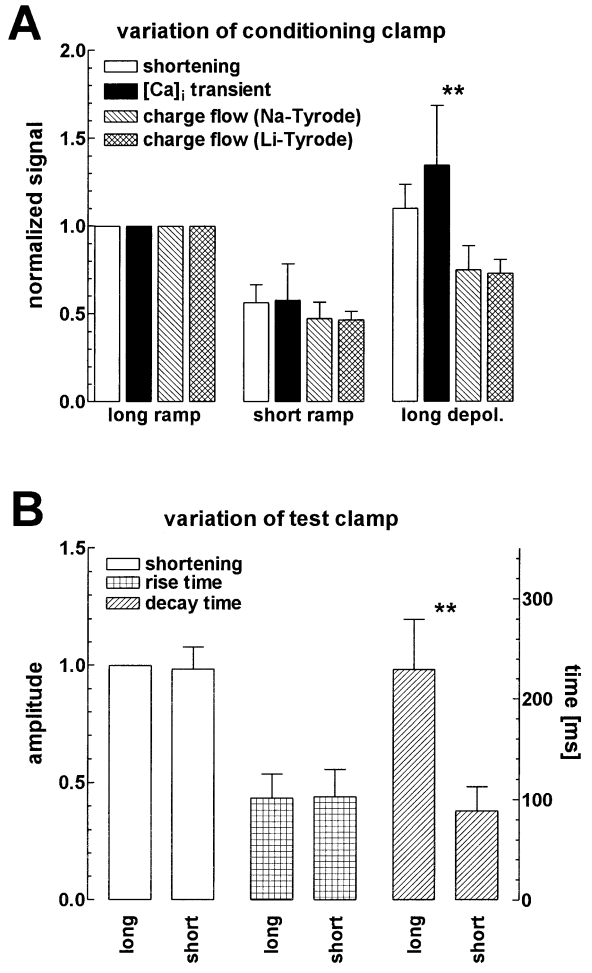

Fig. 7. A Influence of the late $I_{Ca,L}$ component on SR Ca^{2+} loading. Quantitative analysis of shortening measurements and $[Ca^{2+}]_i$ recordings of the types shown in Figs. 4, 5. The relative shortening amplitude during the test clamp (n=17), the integral of the intracellular transient elicited by caffeine discharge of the SR (n=9), and the amount of Ca^{2+} carried by $I_{Ca,L}$ during the conditioning clamps in normal ("*Na-Tyrode*"; n=17) and Na-free Tyrode's solution ("*Li-Tyrode*"; n=8) are displayed. All values were normalized to the respective values measured when AP-like clamps with a repolarizing ramp of 0.2 mV/ms ("*long ramp*"; see Figs. 4A, 5A) were used as conditioning clamps. "*Short ramp*": repolarization rate: 0.77 mV/ms (see Figs. 4B, 5B). "*Long depol.*": combination of a 365-ms square pulse and a ramp clamp with a repolarization rate of 0.77 mV/ms (see Figs. 4C, 5C). Stimulation frequency was 1 Hz, except for the experiments with Na^+-free Tyrode's solution. Since Na^+/Ca^{2+} exchange was blocked under these conditions, stimulation frequency was reduced to 0.2 Hz to avoid Ca^{2+} overload of the cells. $^{**}P<0.0001$ (one-way ANOVA). **B** Influence of the late $I_{Ca,L}$ component on triggering and time course of contraction. Shortening measurements of the type shown in Fig. 6 were analysed. The effect of varying the late component of $I_{Ca,L}$ during the test clamp on relative cell shortening amplitude (*left axis*), rise time, and 10% to 90% decay time of the shortening signal (*right axis*) was investigated. n=14. $^{**}P<0.0001$ (Student's t-test)

change [5, 32], changes in the late $I_{Ca,L}$ component induced by changes in AP duration are another mechanism affecting inotropism. In rat ventricular myocytes Clark and coworkers [12] demonstrated that doubling the charge carried by $I_{Ca,L}$ increased the shortening amplitude by approximately 200%. The differences between the guinea-pig and rat might result from the significantly different AP courses in both species. In addition, Ca^{2+} loading of the SR in guinea-pig ventricular cells depends more on Ca^{2+} entry from the extracellular space than that of rat cells [11, 37]. This might explain why the amount of Ca^{2+} influx via $I_{Ca,L}$ is higher in the guinea-pig than in the rat [1, 6, 13]. Nevertheless, changes in Na^+/Ca^{2+} exchange also influence the SR Ca^{2+} content in guinea-pig ventricular myocytes at least under conditions that slow the forward mode or favour reverse-mode Na^+/Ca^{2+} exchange, as, for example, during delayed repolarization. This was shown by means of AP-like clamp pulses which depolarized the cells for 365 ms to 50 mV (Fig. 4C). Under these conditions Ca^{2+}-charge flow and SR Ca^{2+} load were not proportional (see Fig. 7A), which suggests that the Na^+/Ca^{2+} exchange influences the SR Ca^{2+} content in guinea-pig ventricular myocytes.

In contrast to its indirect function in influencing contraction via changes in SR Ca^{2+} content, the late $I_{Ca,L}$ component had only a minor direct influence on the course of the accompanied cell shortening. Changes in the amount of Ca^{2+} influx carried by late $I_{Ca,L}$ did not affect the rising phase and the amplitude of the simultaneous shortening, although it might change the time course of relaxation. Comparable results were obtained by Beuckelmann and Wier [4] using rectangular voltage-clamp pulses. They found that an increase in depolarizing rectangular voltage-clamp pulses to more than 10–20 ms did not lead to a further increase in the amplitude of $[Ca^{2+}]_i$ transients but only to its prolongation. However, under artificial conditions, when the late component of $I_{Ca,L}$ is elicited after the cell has been depolarized for a longer period (see conditioning clamps in Fig. 4C), the late component was capable of triggering a contraction.

Conclusion

The slow late component of $I_{Ca,L}$, which carries more than 90% of the total amount of Ca^{2+} entering the cell through L-type channels during an AP, is mainly determined by Ca^{2+}-dependent processes. Our observations directly demonstrate that the main function of this current component is to supply Ca^{2+} for SR loading. It is not, however, the only process controlling the SR Ca^{2+} content, which represents the balance of all Ca^{2+} current and Ca^{2+} transport systems. In contrast to its contribution to Ca^{2+} loading, the late $I_{Ca,L}$ component does not appear to be involved in the triggering of contraction under physiological conditions. This function may be linked to the fast early component of $I_{Ca,L}$ [16, 18, 38] or to Ca^{2+} entry by to reverse-mode Na^+/Ca^{2+} exchange [26, 27, 31].

Acknowledgements Part of the experiments were carried out while K.W.L. held a scholarship from the Graduiertenförderung of Northrhine-Westphalia. We are grateful to Dr. David Rosenblatt for critically reading this manuscript. Parts of this paper have been presented at the Meeting of the Physiological Society, Bristol, UK, September 1997 and were published as an abstract: Meyer R, Linz KW (1997), *J Physiol (Lond)* 504:80P.

References

1. Arreola J, Dirksen RT, Shieh RC, Williford DJ, Sheu SS (1991) Ca^{2+} current and Ca^{2+} transients under action potential clamp in guinea pig ventricular myocytes. Am J Physiol 261: C393–C397
2. Barry WH, Bridge JH (1993) Intracellular calcium homeostasis in cardiac myocytes. Circulation 87:1806–1815
3. Bechem M, Pott L (1985) Removal of Ca current inactivation in dialysed guinea-pig atrial cardioballs by Ca chelators. Pflügers Arch 404:10–20
4. Beuckelmann DJ, Wier WG (1988) Mechanism of release of calcium from sarcoplasmic reticulum of guinea-pig cardiac cells. J Physiol (Lond) 405:233–255
5. Bouchard RA, Clark RB, Giles WR (1993) Regulation of unloaded cell shortening by sarcolemmal sodium-calcium exchange in isolated rat ventricular myocytes. J Physiol (Lond) 469:583–599
6. Bouchard RA, Clark RB, Giles WR (1995) Effects of action potential duration on excitation-contraction coupling in rat ventricular myocytes. Action potential voltage-clamp measurements. Circ Res 76:790–801
7. Callewaert G (1992) Excitation-contraction coupling in mammalian cardiac cells. Cardiovasc Res 26:923–932
8. Campbell DL, Giles W (1990) Calcium currents. In: Langer GA (ed) Calcium and the heart. Raven, New York, pp 27–83
9. Campbell DL, Giles WR, Hume JR, Noble D, Shibata EF (1988) Reversal potential of the calcium current in bull-frog atrial myocytes. J Physiol (Lond) 403:267–286
10. Campbell DL, Giles WR, Hume JR, Shibata EF (1988) Inactivation of calcium current in bull-frog atrial myocytes. J Physiol (Lond) 403:287–315
11. Chiesi M, Wrzosek A, Grueninger S (1994) The role of the sarcoplasmic reticulum in various types of cardiomyocytes. Mol Cell Biochem 130:159–171
12. Clark RB, Bouchard RA, Giles WR (1996) Action potential duration modulates calcium influx, Na^{+}-Ca^{2+} exchange, and intracellular calcium release in rat ventricular myocytes. Ann NY Acad Sci 779:417–429
13. Doerr T, Denger R, Doerr A, Trautwein W (1990) Ionic currents contributing to the action potential in single ventricular myocytes of the guinea pig studied with action potential clamp. Pflügers Arch 416:230–237
14. Earm YE, Ho WK, So IS (1990) Inward current generated by Na-Ca exchange during the action potential in single atrial cells of the rabbit. Proc R Soc Lond Ser B Biol Sci 240:61–81
15. Egan TM, Noble D, Noble SJ, Powell T, Spindler AJ, Twist VW (1989) Sodium-calcium exchange during the action potential in guinea-pig ventricular cells. J Physiol (Lond) 411:639–661
16. Fabiato A (1985) Simulated calcium current can both cause calcium loading in and trigger calcium release from the sarcoplasmic reticulum of a skinned canine cardiac Purkinje cell. J Gen Physiol 85:291–320
17. Giles W, Shimoni Y (1989) Slow inward tail currents in the rabbit cardiac cells. J Physiol (Lond) 417:447–463
18. Grantham CJ, Cannell MB (1996) Ca^{2+} influx during the cardiac action potential in guinea pig ventricular myocytes. Circ Res 79:194–200
19. Grynkiewicz G, Poenie M, Tsien RY (1985) A new generation of Ca^{2+} indicators with greatly improved fluorescence properties. J Biol Chem 260:3440–3450
20. Hadley RW, Hume JR (1987) An intrinsic potential-dependent inactivation mechanism associated with calcium channels in guinea-pig myocytes. J Physiol (Lond) 389:205–222.
21. Hamill OP, Marty A, Neher E, Sakmann B, Sigworth FJ (1981) Improved patch-clamp techniques for high-resolution current recording from cells and cell-free membrane patches. Pflügers Arch 391:85–100
22. Imoto Y, Ehara T, Goto M (1985) Calcium channel currents in isolated guinea-pig ventricular cells superfused with Ca-free EGTA solution. Jpn J Physiol 35:917–932
23. Janvier NC, Harrison SM, Boyett MR (1997) The role of inward Na^{+}-Ca^{2+} exchange current in the ferret ventricular action potential. J Physiol (Lond) 498:611–625
24. Kass RS, Sanguinetti MC (1984) Inactivation of calcium channel current in the calf cardiac Purkinje fiber. Evidence for voltage- and calcium-mediated mechanisms. J Gen Physiol 84:705–726
25. Lee KS, Marban E, Tsien RW (1985) Inactivation of calcium channels in mammalian heart cells: joint dependence on membrane potential and intracellular calcium. J Physiol (Lond) 364:395–411
26. Levesque PC, Leblanc N, Hume JR (1994) Release of calcium from guinea pig cardiac sarcoplasmic reticulum induced by sodium-calcium exchange. Cardiovasc Res 28:370–378
27. Levi AJ, Spitzer KW, Kohmoto O, Bridge JH (1994) Depolarization-induced Ca entry via Na-Ca exchange triggers SR release in guinea pig cardiac myocytes. Am J Physiol 266:H1422–H1433
28. Levi AJ, Hancox JC, Howarth FC, Crocker J, Vinnicombe J (1996) A method for making rapid changes of the superfusate whilst maintaining temperature at 37°C. Pflügers Arch 432: 930–937
29. Levi AJ, Mitcheson JS, Hancox JC (1996) The effect of internal sodium and caesium on phasic contraction of patch-clamped rabbit ventricular myocytes. J Physiol (Lond) 492:1–19
30. Linz KW, Meyer R (1997) Modulation of L-type calcium current by internal potassium in guinea pig ventricular myocytes. Cardiovasc Res 33:110–122
31. Lipp P, Niggli E (1994) Sodium current-induced calcium signals in isolated guinea-pig ventricular myocytes. J Physiol (Lond) 474:439–446
32. London B, Krueger JW (1986) Contraction in voltage-clamped, internally perfused single heart cells. J Gen Physiol 88:475–505
33. Matsuda H (1986) Sodium conductance in calcium channels of guinea-pig ventricular cells induced by removal of external calcium ions. Pflügers Arch 407:465–475
34. McDonald TF, Cavalie A, Trautwein W, Pelzer D (1986) Voltage-dependent properties of macroscopic and elementary calcium channel currents in guinea pig ventricular myocytes. Pflügers Arch 406:437–448
35. McDonald TF, Pelzer S, Trautwein W, Pelzer DJ (1994) Regulation and modulation of calcium channels in cardiac, skeletal, and smooth muscle cells. Physiol Rev 74:365–507
36. Meyer R, Wiemer J, Dembski J, Haas HG (1987) Photoelectric recording of mechanical responses of cardiac myocytes. Pflügers Arch 408:390–394
37. Mitchell MR, Powell T, Terrar DA, Twist VW (1987) Electrical activity and contraction in cells isolated from rat and guinea-pig ventricular muscle: a comparative study. J Physiol (Lond) 391:527–544
38. Morad M, Cleemann L (1987) Role of Ca^{2+} channel in development of tension in heart muscle. J Mol Cell Cardiol 19:527–553
39. Näbauer M, Callewaert G, Cleemann L, Morad M (1989) Regulation of calcium release is gated by calcium current, not gating charge, in cardiac myocytes. Science 244:800–803
40. Stegemann M, Meyer R, Haas HG, Robert Nicoud M (1990) The cell surface of isolated cardiac myocytes – a light microscope study with use of fluorochrome-coupled lectins. J Mol Cell Cardiol 22:787–803
41. Terracciano CM, Tweedie D, MacLeod KT (1997) The effects of changes to action potential duration on the calcium content of the sarcoplasmic reticulum in isolated guinea-pig ventricular myocytes. Pflügers Arch 433:542–544
42. Wang SY, Dong L, Langer GA (1997) Matching Ca efflux and influx to maintain steady-state levels in cultured cardiac cells. Flux control in the sarcolemmal cleft. J Mol Cell Cardiol 29:1277–1287
43. Wasserstrom JA, Vites AM (1996) The role of Na^{+}-Ca^{2+} exchange in activation of excitation-contraction coupling in rat ventricular myocytes. J Physiol (Lond) 493:529–542